

Cite this: *Chem. Sci.*, 2025, 16, 11908

All publication charges for this article have been paid for by the Royal Society of Chemistry

Received 18th April 2025  
Accepted 20th May 2025

DOI: 10.1039/d5sc02836a

rsc.li/chemical-science

## Photocatalytic synthesis of 2-oxabicyclo[2.1.1]hexanes: cobalt-enhanced efficiency†

Si-Yuan Tang,<sup>‡a</sup> Zhan-Jie Wang,<sup>‡a</sup> Jin-Jiao Wu,<sup>a</sup> Zhi-Xi Xing,<sup>a</sup> Ze-Yi Du<sup>b</sup> and Huan-Ming Huang<sup>\*,a</sup>

Development of new synthetic strategies to prepare C(sp<sup>3</sup>)-rich arene bioisosteres, especially their heteroatom incorporating analogs, is less explored, but highly in demand. Here we report a photocatalytic [2π + 2σ] cycloaddition reaction between bicyclo[1.1.0]butanes and aldehydes enabled by cobalt under visible light irradiation. The key step is that bicyclo[1.1.0]butanes could be oxidized to generate radical cation intermediates which could be promoted by cobalt, facilitating a nucleophilic addition to the aldehydes. This unprecedented strategy exhibits broad functional group tolerance and efficiently constructs complex molecular architectures and derivatives of natural products with good to excellent yields. Detailed mechanistic studies and product manipulation have demonstrated the viability of this open-shell approach. The desired 2-oxa-BCH motif demonstrated excellent acidity tolerance and significantly enhanced lipophilicity potentially leading to enhanced metabolic properties and *in vitro* bioactivities compared to its parent phenyl-type bioisostere.

### Introduction

The phenyl ring is a prevalent functional group in pharmaceuticals and materials science.<sup>1</sup> In recent years, the concept of “escaping from flatland” has gained traction among medicinal and synthetic chemists,<sup>2</sup> prompting the exploration of novel synthetic methods to create conformationally rigid structures characterized by a higher content of sp<sup>3</sup>-hybridized carbon atoms compared to traditional arenes.<sup>3</sup> Notable examples of such structures include bicyclo[1.1.1]pentanes (BCPs),<sup>4</sup> bicyclo[2.1.1]hexanes (BCHs),<sup>5</sup> and bicyclo[3.1.1]heptanes (BCHeps).<sup>6</sup> In recent developments, Mykhailiuk and colleagues demonstrated that C(sp<sup>3</sup>)-rich arene bioisosteres incorporating heteroatoms could potentially replace medicinally relevant heteroaromatic rings while offering enhanced properties such as better aqueous solubility, improved metabolic stability, and reduced lipophilicity.<sup>7</sup> However, synthetic approaches for such bioisosteres have been less thoroughly explored. Traditionally, 2-oxabicyclo[2.1.1]hexanes (2-oxa-BCHs) are synthesized using classical photochemical [2 + 2] reactions (Fig. 1A), yet these methods

often come with limitations in terms of substrate scope and functional group compatibility.<sup>8</sup>

Recently, strain-release cycloaddition between bicyclo[1.1.0]butanes (BCBs) and aldehydes has advanced as a promising approach to construct 2-oxabicyclo[2.1.1]hexanes (2-oxa-BCHs) (Fig. 1B).<sup>9</sup> Notably, Glorius and co-workers developed two elegant synthetic approaches for 2-oxa-BCHs using energy transfer catalysis (Fig. 1B, I)<sup>10a</sup> or Lewis acid catalysis (Fig. 1B, II),<sup>10b</sup> respectively. Moreover, recent advancements by researchers such as Zi,<sup>11a</sup> Zheng,<sup>11b</sup> and Yang<sup>11c</sup> have demonstrated the use of palladium catalysis to synthesize 2-oxa-BCHs from vinylbicyclo[1.1.0]butanes (VBCBs) and carbonyl compounds (Fig. 1B, III). Glorius and co-workers developed dearomative cycloaddition reactions<sup>12a</sup> and [2π + 2σ] cycloaddition<sup>12b</sup> to afford various BCHs through oxidative activation of ester-substituted BCBs. During the investigation for our research, we found that Walker and his team demonstrated an elegant example of formal [2π + 2σ] cycloaddition between BCBs and alkenes or aldehydes using a simple photoredox catalyst under visible light, although they faced challenges related to relatively low yields and limited substrate scope for oxa-BCHs (Fig. 1B, IV).<sup>13</sup> Additionally, Leitch,<sup>14a</sup> Glorius,<sup>14b-e</sup> Mykhailiuk,<sup>7c</sup> Feng,<sup>14f-i</sup> Li,<sup>14j</sup> Wang & Li,<sup>14k</sup> Zheng,<sup>14l</sup> Deng,<sup>14m</sup> Aggarwal,<sup>14n</sup> Zhou,<sup>14o</sup> Studer,<sup>14p</sup> and many others<sup>9</sup> introduced several synthetic strategies towards the synthesis of C(sp<sup>3</sup>)-rich arene bioisosteres incorporating heteroatoms successfully.

Inspired by these elegant examples and our recent achievements<sup>15</sup> in the area of radical-polar chemistry,<sup>16</sup> we disclose a rare example of the photocatalytic synthesis of

<sup>a</sup>School of Physical Science and Technology, ShanghaiTech University, Shanghai 201210, China. E-mail: huanghm@shanghaitech.edu.cn

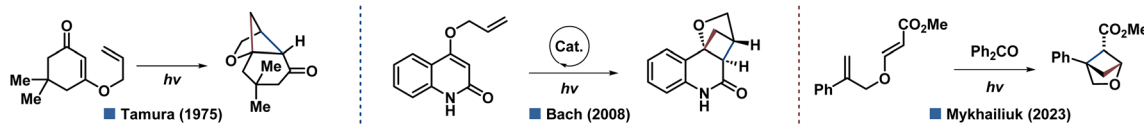
<sup>b</sup>Department of Medicinal Chemistry, School of Pharmacy, Fudan University, No. 826 Zhangheng Road, Shanghai 201203, China

† Electronic supplementary information (ESI) available. CCDC 2389698. For ESI and crystallographic data in CIF or other electronic format see DOI: <https://doi.org/10.1039/d5sc02836a>

‡ These authors contributed equally to this work.



## A. Representative examples to access 2-oxabicyclo[2.1.1]hexanes through photochemical [2+2] reactions



## B. Recent synthetic approaches regarding 2-oxabicyclo[2.1.1]hexanes synthesis

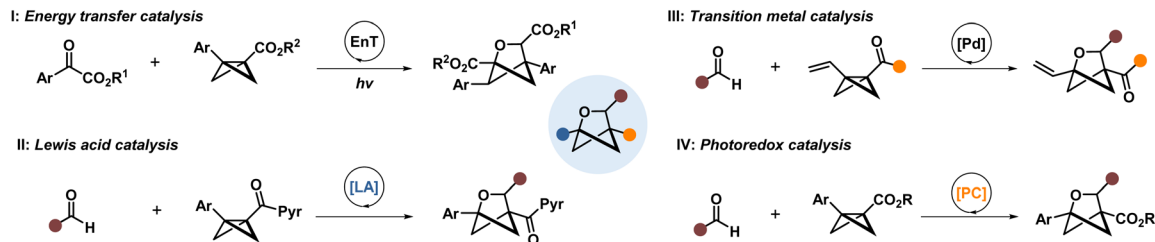
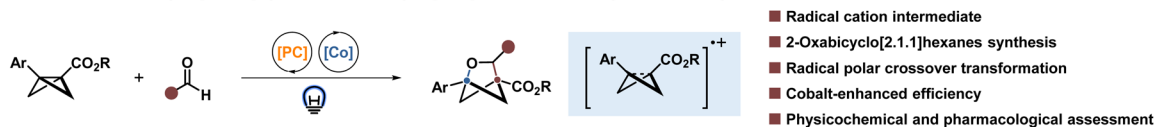
C. **This work:** Photocatalytic  $[2\pi+2\sigma]$  cycloaddition of bicyclo[1.1.0]butanes with aldehydes enabled by cobalt

Fig. 1 Background and rational design. (A) Representative examples to access 2-oxabicyclo[2.1.1]hexanes through photochemical [2 + 2] reactions. (B) Recent synthetic approaches regarding 2-oxabicyclo[2.1.1]hexanes synthesis. (C) This work: photocatalytic  $[2\pi + 2\sigma]$  cycloaddition of bicyclo[1.1.0]butanes with aldehydes enabled by cobalt.

2-oxa-BCHs by coupling bicyclo[2.1.1]hexenes (BCBs) with aldehydes, promoted by cobalt under visible light conditions (Fig. 1C). Our approach involves the oxidation of BCBs by strongly oxidative photoredox catalysis to generate radical cation intermediates under visible light conditions. These intermediates could be promoted by cobalt, which facilitates nucleophilic addition to both aromatic and aliphatic aldehydes.

## Results and discussion

### Reaction design and optimization

With this in mind, we investigated the coupling reaction between BCBs **1a** and aliphatic aldehyde **2a**, and we successfully formed the desired 2-oxa-BCHs **3** with a 90% isolated yield using 1 mol% of photocatalyst **PC1** and 7.5 mol%  $\text{CoCl}_2$  in dichloroethane (DCE), under the irradiation of 450 nm LEDs for 12 hours (Table 1, entry 1). We screened several photocatalysts and found that a highly oxidative photocatalyst is crucial for achieving high yields (entries 2–5). Increasing the amounts of either the photocatalyst or the cobalt catalyst resulted in lower yields (entries 6–10). We also explored the impact of the DCE concentration (entries 11 and 12), the addition of various additives (entries 13 and 14), changing solvents (entries 15–17), and varying reaction times (entries 18 and 19), all of which led to decreased yields. Control experiments demonstrated the necessity of visible light, the photocatalyst, and the cobalt

catalyst to achieve excellent yields (entries 20–24). Notably, the absence of the cobalt catalyst resulted in only a 56% isolated yield, highlighting its importance for optimal yield (entry 23).

### Substrate scope

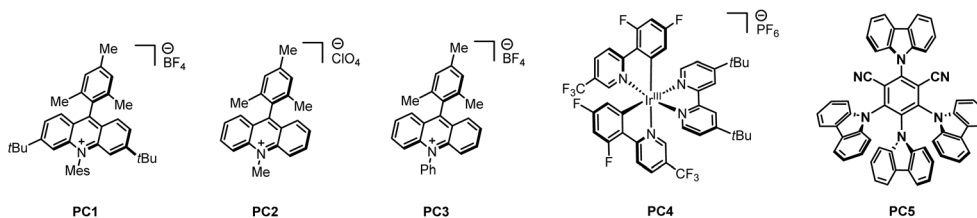
With the optimized conditions established, we began to explore the substrate scope using various aliphatic aldehydes (Fig. 2). The reaction conditions were found to be compatible with a range of functional groups on the aromatic ring, including fluoro (**4**), chloro (**5**), methyl (**6**), *tert*-butyl (**7**), and methoxy (**8**). The absence of a cobalt catalyst resulted in significantly reduced or trace yields of the desired products (**4**–**5**). We further investigated a variety of aliphatic aldehydes, such as ethyl (**9**), benzyl (**10** and **16**), cyclopropyl (**11**), cyclobutyl (**12**), cyclopentyl (**13**), cyclohexyl (**14**–**15**), isopropyl (**16** and **20**), protected alcohols (**18** and **21**), and esters (**19** and **24**–**25**), as well as chloro (**22**). Our method was then successfully applied to the synthesis of drug-related 2-oxa-BCHs, derived from various aliphatic aldehydes, such as those in fenbufen (**26**), flurbiprofen (**27**), aspirin (**28**), ketoprofen (**29**), ibuprofen (**30**), isoxepac (**31**), and valproate (**32**).

We then proceeded to explore various aromatic aldehydes and BCHs (Fig. 3). The newly developed catalytic system successfully tolerated simple phenyl aldehyde, yielding the desired 2-oxa-BCH **33** with an 85% isolated yield, as confirmed by X-ray analysis (CCDC 2389698). A range of functional groups



Table 1 Optimization table<sup>a</sup>

Entry	Variation from the “optimized conditions”	Isolated yield [%]
1	<b>None</b>	<b>90</b>
2	<b>PC2</b> instead of <b>PC1</b>	ND
3	<b>PC3</b> instead of <b>PC1</b>	50
4	<b>PC4</b> instead of <b>PC1</b>	ND
5	<b>PC5</b> instead of <b>PC1</b>	ND
6	2 mol% <b>PC1</b>	84
7	10 mol% $\text{CoCl}_2$	84
8	1 eq. of $\text{CoCl}_2$	75
9	$\text{CoI}_2$ instead of $\text{CoCl}_2$	ND
10	$\text{CoCl}_2 \cdot 6\text{H}_2\text{O}$ instead of $\text{CoCl}_2$	75
11	Concentration: 0.4 M	75
12	Concentration: 0.1 M	73
13	1 eq. of $\text{K}_2\text{CO}_3$ as an additive	ND
14	1 eq. of collidine as an additive	ND
15	DCM instead of DCE	87
16	MeCN instead of DCE	ND
17	THF instead of DCE	ND
18	18 h instead of 12 h	87
19	6 h instead of 12 h	78
20	No <b>PC1</b> , $\text{CoCl}_2$ (7.5 mol%)	ND
21	No <b>PC1</b> , $\text{CoCl}_2$ (1 eq.)	6
22	No light at 40 °C	ND
23	No $\text{CoCl}_2$	56
24	No <b>PC1</b> and $\text{CoCl}_2$	ND



<sup>a</sup> Reaction conditions:  $\text{CoCl}_2$  (7.5 mol%),  $\text{Mes}_2\text{Acr-tBu}_2\text{BF}_4$  (**PC1**, 1 mol%), freshly prepared BCB **1a** (0.2 mmol, 2 equiv.) and aldehyde **2a** (0.1 mmol, 1 equiv.) were dissolved in DCE (0.5 mL, 0.2 M). The mixture was irradiated with 30 W 450 nm blue LEDs with a cooling fan for 12 h under  $\text{N}_2$ .

on the aromatic ring were also examined, including methyl (**34**), phenyl (**35**), fluoro (**36**, **46–47**), chloro (**37**), bromo (**38**), trifluoromethyl (**39**), phenoxy (**40**), *tert*-butyl (**41**), methoxy (**42–45**), benzofuran (**48**), and bicyclic aromatic rings (**49**), all of which were tolerated, resulting in isolated yields of 58–79%. Various BCBs were screened as well, including those with substituted aromatic rings, such as methyl (**50–52**), fluoro (**53**), chloro (**54**), and naphthyl (**55**). The desired 2-oxa-BCHs were obtained in moderate to excellent yields. Additionally, different ester groups were investigated, including complex motifs such as *L*-menthol

(**58**) and pregnenolone (**59**). The desired 2-oxa-BCHs (**56–59**) were obtained in good yields. Notably, the reactions involving BCBs with ester groups resulted in very low yields (30% NMR yield) when catalysed by Lewis acid,<sup>10b</sup> highlighting the unique efficacy of cobalt.

### Mechanistic studies and the proposed mechanism

With a relatively broad substrate scope established, we began to explore the reaction mechanism through radical cation



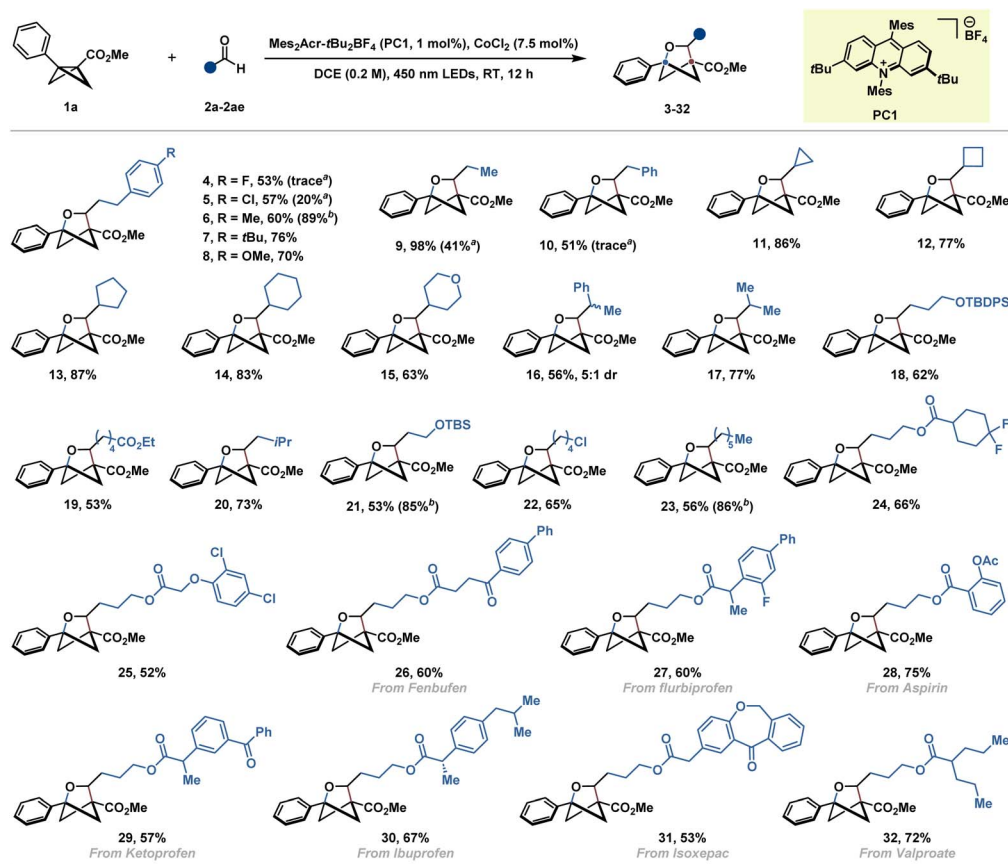


Fig. 2 Substrate scope regarding various aliphatic aldehydes. Reaction conditions:  $\text{CoCl}_2$  (7.5 mol%),  $\text{Mes}_2\text{Acr-tBu}_2\text{BF}_4$  (PC1, 1 mol%), freshly prepared BCB **1a** (0.2 mmol, 2 equiv.) and aldehyde **2** (0.1 mmol, 1 equiv.) were dissolved in DCE (0.5 mL, 0.2 M). The mixture was irradiated with 30 W 450 nm blue LEDs with a cooling fan for 12 h under  $\text{N}_2$ . <sup>a</sup>No  $\text{CoCl}_2$  under optimized conditions; <sup>b</sup>3 equiv. of **1a** was used.

trapping experiments (Fig. 4A). Under an oxygen atmosphere using the dual catalytic system, the epoxide derivative **60** was obtained in a 21% isolated yield, suggesting the presence of a radical cation intermediate.<sup>17</sup> Additionally, this intermediate was trapped by methanol, yielding the corresponding product **61** in a 30% isolated yield. Further evidence supporting the involvement of radical intermediates came from the detection and isolation of a PBN adduct **62** and a TEMPO adduct **63** (Fig. 4B). We also utilized the aliphatic aldehyde **2x**, which contains a three-membered ring, and the desired 2-oxa-BCH **64** was formed smoothly. This outcome suggests that a ketyl radical is not formed in our catalytic system (Fig. 4C). After screening alternative transition metal additives, we determined that  $\text{CoCl}_2$  remains the most effective for achieving a high yield of **3** (Fig. 4D). Stern–Volmer and UV-vis experiments were conducted, clearly indicating that only the photocatalyst (PC1,  $\text{Mes}_2\text{Acr-tBu}_2\text{BF}_4$ ) absorbs the visible light (Fig. 4F) and that only BCBS **2a** quenched the photoexcited PC1 (Fig. 4E). The quantum yield of this dual catalytic system was measured, and the result ( $\phi = 0.16$ ) suggests that a radical chain mechanism is unlikely.

Based on these mechanistic studies (Fig. 4G), we propose that BCB **2a** (+1.79 V vs.  $\text{Ag}/\text{AgCl}$ )<sup>12b</sup> could be oxidized by PC1, ( $E[\text{PC}^*/\text{PC}^{\cdot-}] = 2.0$  V vs. SCE)<sup>18</sup> to generate the radical cation intermediate **II**. This intermediate can be reduced to intermediate **III** and its tautomer **IV** by the reduced form of PC1,<sup>19</sup> which is then trapped by aldehyde **2a** to form intermediate **V**. The final 2-oxa-BCHs **3** is produced after ring closure, completing the photocatalytic cycle. Alternatively, radical cation intermediate **II** could be promoted by cobalt(II), generating intermediate **VI** and its tautomer **VII**. A Reformatsky-type addition to aliphatic aldehyde **2a** efficiently forms intermediate **V**, leading to the final 2-oxa-BCHs **3**. The  $\text{Co(II)}$  could be reduced back to  $\text{Co(I)}$  by the reduced PC1, allowing both catalytic cycles to turn over efficiently.<sup>20,21</sup>

### Synthetic application and pharmacological activity of 2-oxa-BCHs

To explore the application of our reaction and the 2-oxa-BCH motif we synthesized, we first tested the model reaction on a gram scale with an excellent 92% yield of 2-oxa-BCHs **3** and



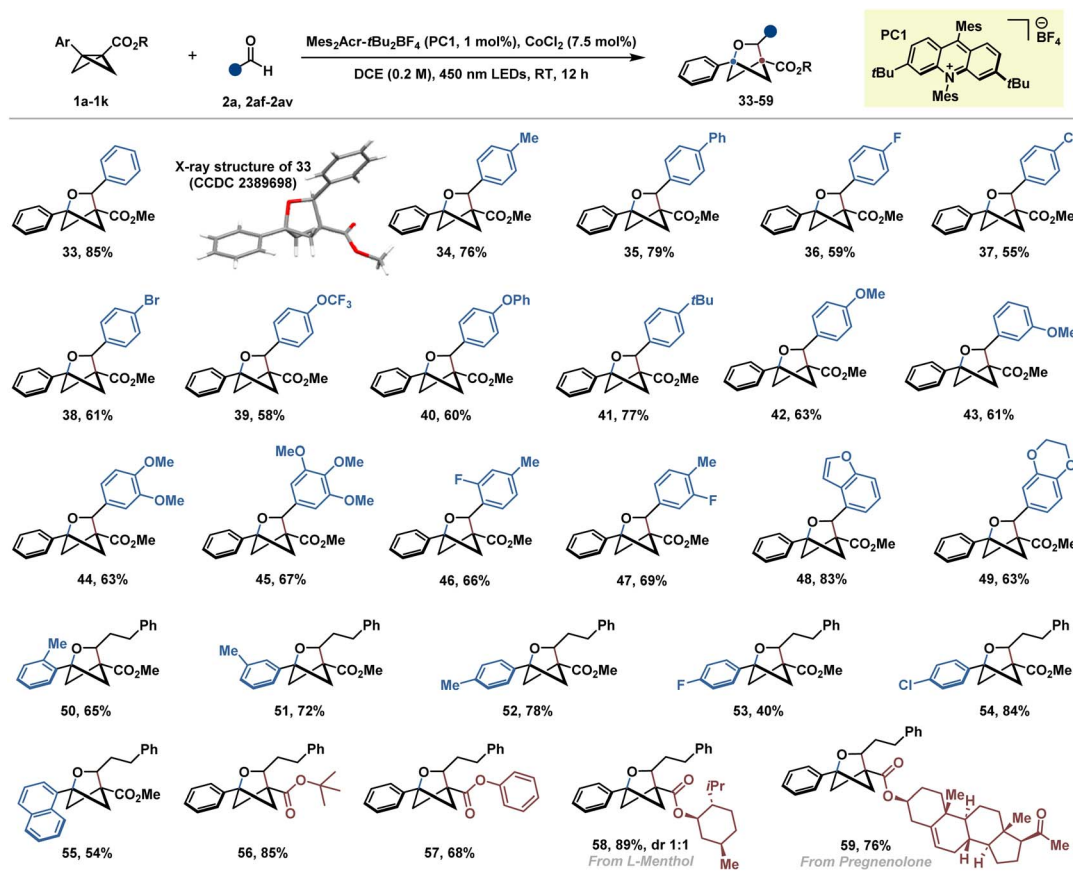


Fig. 3 Substrate scope regarding various BCBs and aldehydes. Reaction conditions:  $\text{CoCl}_2$  (7.5 mol%),  $\text{Mes}_2\text{Acr-tBu}_2\text{BF}_4$  (PC1, 1 mol%), freshly prepared BCB **1** (0.2 mmol, 2 equiv.) and aldehyde **2** (0.1 mmol, 1 equiv.) were dissolved in DCE (0.5 mL, 0.2 M). The mixture was irradiated with 30 W 450 nm blue LEDs with a cooling fan for 12 h under  $\text{N}_2$ .

diverse manipulation could be achieved (Fig. 5A). The ester group in **3** can be transferred to the corresponding amide **65**. Alternatively, 2-oxa-BCHs **3** can be reduced to alcohol **66**, which could then be converted to azide **67**. Additionally, the ester group in **3** could be easily hydrolyzed under basic conditions to yield the corresponding carboxylic acid **68** with excellent yield. Different tertiary alcohols such as **69** and **70** could be obtained from **3** through MeLi nucleophilic addition or the Kulinkovich reaction. Finally, two different drug derivatives **71** and **72** could be synthesized from atomoxetine and leelamine *via* amide coupling and the ammonolysis reaction to further evaluate the physicochemical properties of our 2-oxa-BCH motif on mature drug scaffolds, therefore assessing the preliminary parameters in drug development such as lipophilicity, acidity and stability.

As shown in Fig. 5B, after introducing the 2-oxa-BCH motif, the lipophilicity of the modified substrates **71** and **72** significantly increased with higher  $C \log P$  and tPSA values. The predicted  $\text{p}K_a$  values for the parent compound atomoxetine and leelamine, as well as their derivatives **71** and **72** also illustrated significant changes.<sup>22</sup> These variations in physicochemical properties are likely to significantly influence the ADME

properties and this hypothesis agreed with the later result when we predicted the stability of four substrates in human plasma by using a published attention-based graph neural network program PredPS.<sup>23</sup> The lower values of **71** and **72** compared to the parent atomoxetine and leelamine suggested improved stability in human plasma. In addition, we practically measure the stability of both **71** and **72** under acidic conditions at 37 °C that simulate the *in vivo* gastric conditions. Under even more acidic conditions than those found in the stomach,<sup>24</sup> both **71** and **72** remained stable after 24 hours in 0.2 M and 2 M HCl, demonstrating the remarkable acidity tolerance of the 2-oxa-BCH motif. Interestingly, the two substrates exhibited different behaviors in concentrated HCl as most of the **71** was hydrolyzed, whereas a significant portion of **72** was still recoverable. This difference was potentially due to that the tertiary amide in **71** was easier to be protonated therefore leading to an acid-promoted hydrolysis. All in all, our 2-oxa-BCH motif could provide different physicochemical properties and illustrate excellent acid tolerance; therefore, we further synthesized **73** and **74** to compare the pharmacological behaviour between our 2-oxa-BCH motif and its parent phenyl bioisostere.



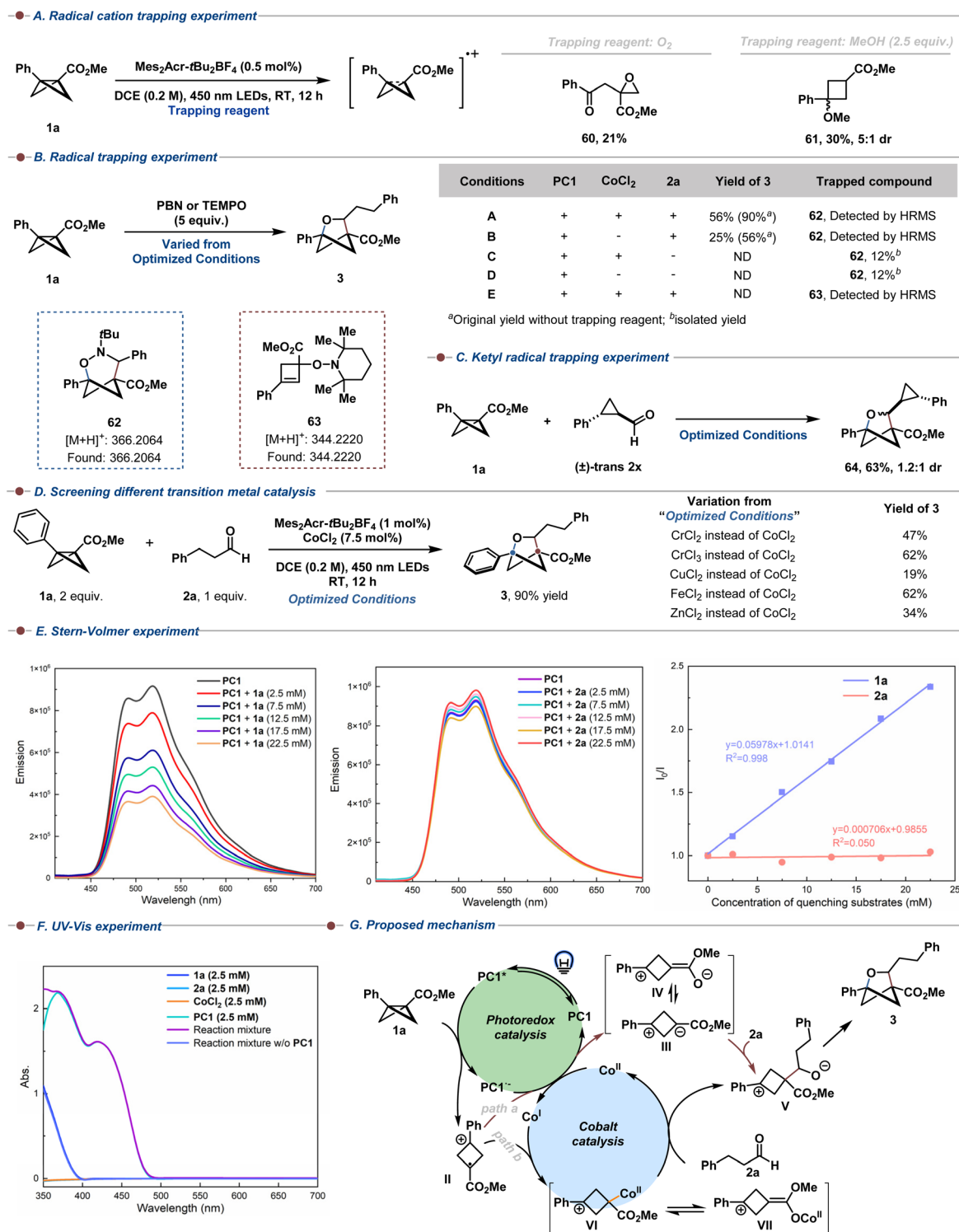


Fig. 4 Mechanistic studies and the proposed mechanism.



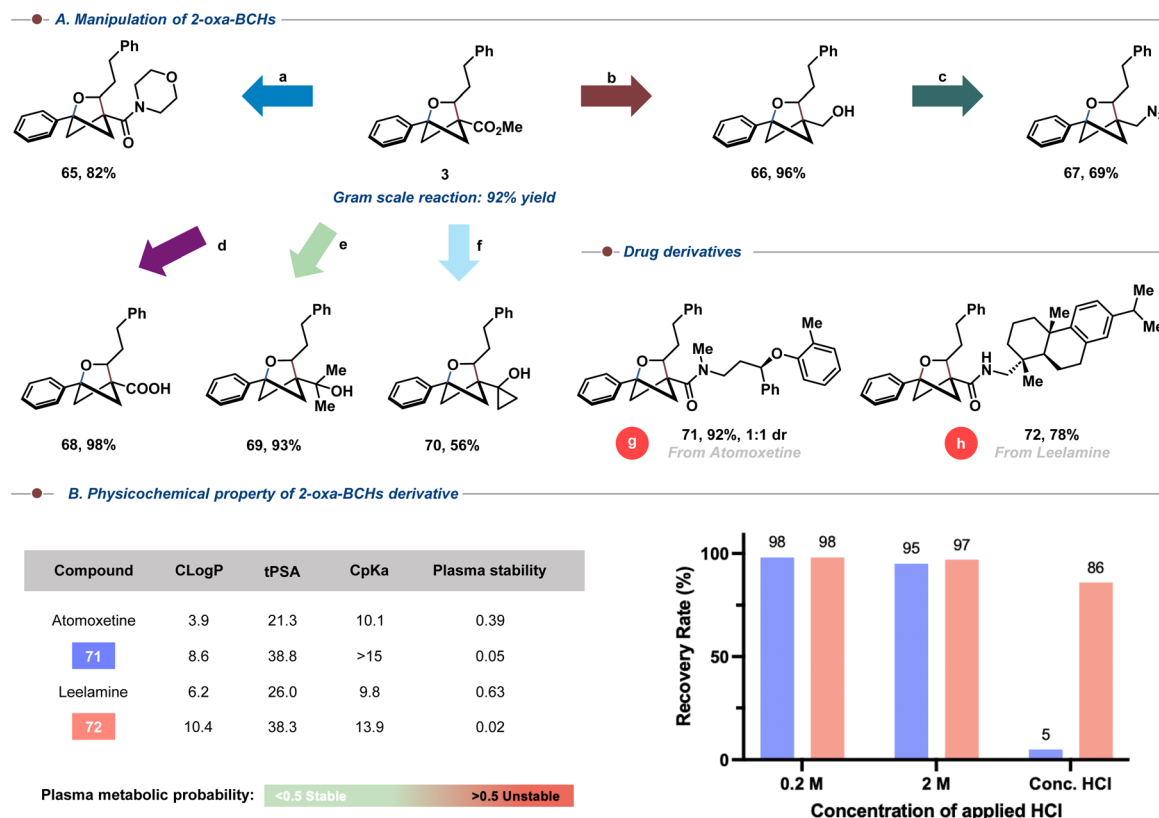


Fig. 5 Synthetic application and physicochemical properties of 2-oxa-BCHs. (A) (a) Morpholine (2 eq.), LiHMDS (2 eq.), toluene, RT, 12 h; (b)  $\text{BH}_3 \cdot \text{THF}$  (2.5 eq.), THF, 65 °C, 12 h; (c) DPPA (2 eq.), DBU (3 eq.), THF, 65 °C, 48 h; (d) NaOH (3 eq.), THF/MeOH/ $\text{H}_2\text{O}$  = 4 : 1 : 1, 50 °C, 6 h; (e) MeLi (2 eq.), THF, 40 °C, 12 h; (f)  $\text{Ti}(\text{OiPr})_4$  (1.4 eq.), EtMgBr (2.8 eq.), THF, RT, 12 h; (g) **68** (1 eq.), atomoxetine (1.2 eq.), EDCI·HCl (1.5 eq.), DMAP (0.2 eq.), DCM, RT, 12 h; (h) **3** (1 eq.), leelamine (5 eq.), LiHMDS (5 eq.), toluene, RT, 12 h. (B) C log P: calculated logarithm of the partition coefficient using ChemDraw Office; tPSA: the calculated topological polar surface area using ChemDraw Office; CpKa: the predicted acid dissociation constant using MolGpKa; plasma stability was predicted using PredPS. Acidity tolerance of **71** and **72** was assessed under indicated acidic conditions at 37 °C for 24 hours by calculating the recovery rate. More details could be found in the ESI.†

As shown in Fig. 6A, our 2-oxa-BCH motif (in cream stick representation) possessed a similar shape compared to its bioisostere (in cyan stick representation) with a comparable bond length and angle. More importantly, the 2-oxa-BCH motif contained oxygen as a hydrogen bond acceptor and possessed a more lipophilic and stereo scaffold, therefore potentially contributing to van der Waals force during binding to the target enzymes and therefore enhancing the pharmacological activities. By measuring the binding affinity of **73** and **74** towards the KOR (Kappa Opioid Receptor), we found that our 2-oxa-BCH motif supplied almost 10 times higher potency compared to the parent bioisostere. To reveal the plausible reasons behind this binding affinity enhancement, we further did the docking analysis of **73** and **74** (Fig. 6B). Both **73** (in cream stick representation, Fig. 6B) and **74** (in cyan stick representation, Fig. 6B) were located at the typical binding pocket of the KOR with similar binding orientations (gray ribbon, Fig. 6B) and conserved interactions between the morphinan of **73** and **74** and the KOR agreed with

the previous report.<sup>25</sup> To be specific, **73** (in cream stick representation, Fig. 6B) and **74** (in cyan stick representation, Fig. 6B) could form a salt bridge towards the KOR between the basic tertiary amine and D138<sup>3.32</sup> (in gray stick representation, Fig. 6B) whereas a hydrogen bond (in the red line, Fig. 6B) was observed through the methoxy group of the substrates to Y139<sup>3.33</sup> (in gray stick representation, Fig. 6B). Lipophilic interactions such as van der Waals forces mainly existed between the phenanthrene and M142<sup>3.36</sup>, V230<sup>5.42</sup> and I290<sup>6.51</sup> (in green stick representation, Fig. 6B), as well as between the cyclopropylmethyl group and W287<sup>6.48</sup> and Y320<sup>7.43</sup> (in purple stick representation, Fig. 6B). In addition, some unique interactions belonging to **73** were observed that could potentially explain its higher potency compared to the parent **74**. Predicted hydrogen bonds between the amide linkage and residues S211<sup>EL2</sup> and Y312<sup>7.24</sup> could be observed (in red lines, Fig. 6B), as well as potential  $\pi$ - $\pi$  stacking interactions between the phenyl group and Y312<sup>7.24</sup> could further enhance the binding affinity. Moreover, the terminal



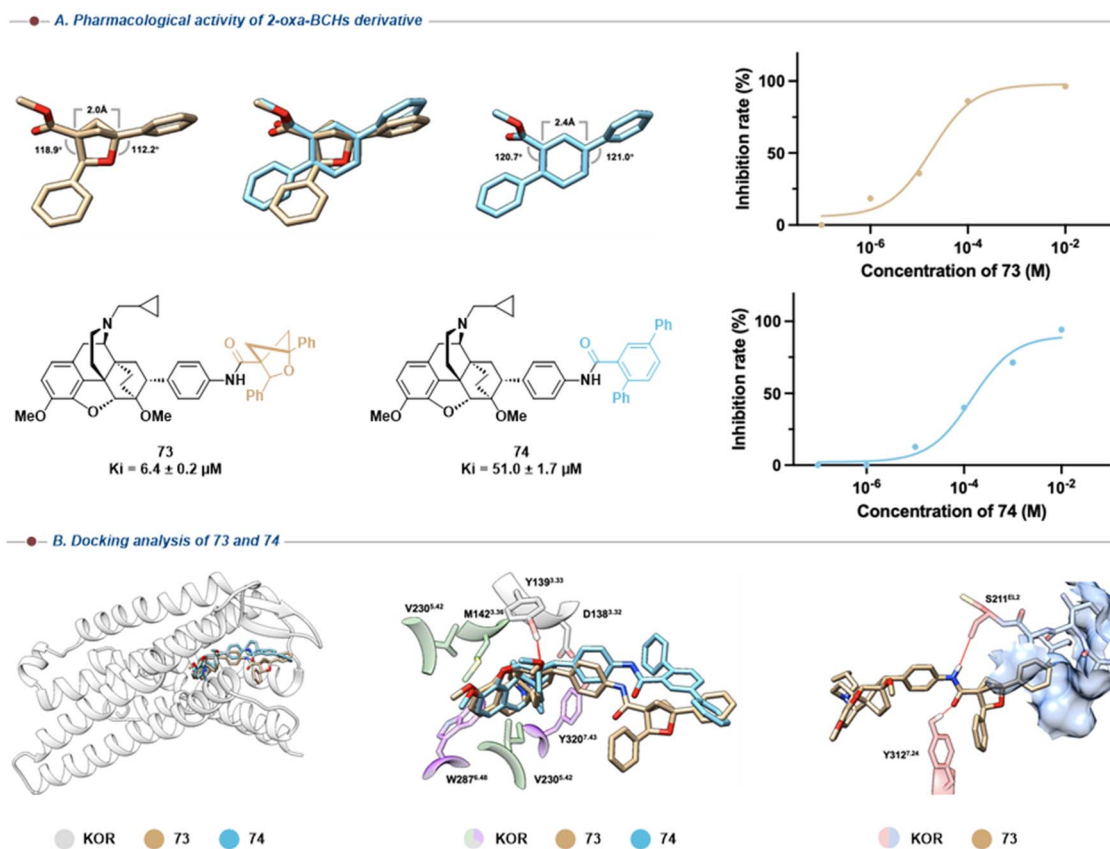


Fig. 6 Pharmacological activity and docking analysis of 2-oxa-BCHs. (A) Structures of compounds **73** and **74**, and their terminal motif comparison (in cream and cyan stick representation respectively) and KOR binding affinity of **73** and **74**. The bond length and angle of the benzene bioisostere were referenced from CCDC 127167. (B) A putative binding mode of compound **73** (in cream stick representation) and **74** (in cyan stick representation) in a complex with the KOR (PDB entry: 6B73). Possible interactions between **73**, **74** and KOR residues; the hydrogen bond (in red lines) and binding surface (in blue surface) were simulated using software Chimera 1.13.1.

phenyl group was located in the lipophilic “sandwich”-shaped pocket (constructed by N122<sup>3,16</sup>, S123<sup>3,17</sup>, I208<sup>EL2</sup>, E209<sup>EL2</sup>, and C210<sup>EL2</sup>) and such plausible van der Waals forces could also contribute to the KOR binding affinity.

## Conclusions

In summary, we have developed a photocatalytic  $[2\pi + 2\sigma]$  cycloaddition reaction between bicyclo[1.1.0]butanes and aldehydes, promoted by cobalt under visible light irradiation. This method enables the formation of a diverse library of 2-oxa-BCHs in good to excellent yields, offering broad substrate scope and functional group tolerance under mild conditions. Key steps in this process include the formation of a radical cation intermediate and enhancement of efficiency using cobalt. The 2-oxa-BCH motif we developed in this work displays not only excellent acidity tolerance but also enhanced substrate–drug target interactions compared to its phenyl-type bioisostere due to its unique chemical features. We anticipate that this new synthetic approach will find further applications in the synthesis of C(sp<sup>3</sup>)-rich arene bioisosteres incorporating different heteroatoms and the 2-oxa-BCH motif holds great potential as a bioisostere for the phenyl motif in future drug design.

## Data availability

Materials and methods, detailed optimization studies, experimental procedures, mechanistic studies and NMR spectra are available in the ESI† and from the corresponding authors upon request.

## Author contributions

H.-M. H. conceived and directed the project; S.-Y. T., Z.-J. W. and Z.-X. X. performed all the experiments and analysed all the data. *In vitro* assays were performed by Z.-Y. D. and molecular modelling studies were conducted by S.-Y. T. and Z.-Y. D. H.-M. H. and S.-Y. T. wrote the manuscript with contributions from all authors.

## Conflicts of interest

There are no conflicts to declare.

## Acknowledgements

We are grateful for financial support from the National Natural Science Foundation of China (22201179 & 22471168 to H.-M.



H.), the startup funding from ShanghaiTech University (H.-M. H.), the Postdoctoral Fellowship Program of CPSF (No. GZC20231674 to S.-Y. T.) and the Double First-Class Initiative Fund of ShanghaiTech University (S.-Y. T.). We sincerely thank Prof. Chaodan Pu, Zhuo Zhao, Shu-Ya Wen and Ying Zhang (all at ShanghaiTech University), Wei Li (Fudan University), and Yujun Wang (Shanghai Institute of Materia Medica) for help with substrate synthesis, mechanistic study, X-ray analysis and drug activity tests.

## Notes and references

- R. D. Taylor, M. Maccoss and A. D. G. Lawson, *J. Med. Chem.*, 2014, **57**, 5845–5859.
- F. Lovering, J. Bikker and C. Humblet, *J. Med. Chem.*, 2009, **52**, 6752–6756.
- (a) M. A. M. Subbaiah and N. A. Meanwell, *J. Med. Chem.*, 2021, **64**, 14046–14128; (b) P. K. Mykhailiuk, *Org. Biomol. Chem.*, 2019, **17**, 2839–2849; (c) J. Tsien, C. Hu, R. R. Merchant and T. Qin, *Nat. Rev. Chem.*, 2024, **8**, 605–627.
- Selected examples, see: (a) B. R. Shire and E. A. Anderson, *JACS Au*, 2023, **3**, 1539–1553; (b) J. M. Anderson, N. D. Measom, J. A. Murphy and D. L. Poole, *Angew. Chem., Int. Ed.*, 2021, **60**, 24754–24769; (c) M. M. D. Pramanik, H. Qian, W. J. Xiao and J. R. Chen, *Org. Chem. Front.*, 2020, **7**, 2531–2537; (d) R. Gianatassio, J. M. Lopchuk, J. Wang, C. Pan, L. R. Malins, L. Prieto, T. A. Brandt, M. R. Collins, G. M. Gallego, N. W. Sach, J. E. Spangler, H. Zhu, J. Zhu and P. S. Baran, *Science*, 2016, **351**, 241–246; (e) X. Zhang, R. T. Smith, C. Le, S. J. McCarver, B. T. Shireman, N. I. Carruthers and D. W. C. MacMillan, *Nature*, 2020, **580**, 220–226; (f) Y. Yang, J. Tsien, J. M. E. Hughes, B. K. Peters, R. R. Merchant and T. Qin, *Nat. Chem.*, 2021, **13**, 950–955; (g) J. H. Kim, A. Ruffoni, Y. S. S. Al-Faiyz, N. S. Sheikh and D. Leonori, *Angew. Chem., Int. Ed.*, 2020, **59**, 8225–8231.
- Selected examples, see: (a) A. Denisenko, P. Garbuz, S. V. Shishkina, N. M. Voloshchuk and P. K. Mykhailiuk, *Angew. Chem., Int. Ed.*, 2020, **59**, 20515–20521; (b) R. Kleinmans, T. Pinkert, S. Dutta, T. O. Paulisch, H. Keum, C. G. Daniliuc and F. Glorius, *Nature*, 2022, **605**, 477–482; (c) S. Agasti, F. Beltran, E. Pye, N. Kaltsoyannis, G. E. M. Crisenza and D. J. Procter, *Nat. Chem.*, 2023, **15**, 535–541; (d) T. Rigotti and T. Bach, *Org. Lett.*, 2022, **24**, 8821–8825; (e) S. Paul, D. Adelfinsky, C. Salome, T. Fessard and M. K. Brown, *Chem. Sci.*, 2023, **14**, 8070–8075; (f) A. Denisenko, P. Garbuz, Y. Makovetska, O. Shablykin, D. Lesyk, G. Al-Maali, R. Korzh, I. V. Sadkova and P. K. Mykhailiuk, *Chem. Sci.*, 2023, **14**, 14092–14099; (g) M. Reinhold, J. Steinebach, C. Golz and J. C. L. Walker, *Chem. Sci.*, 2023, **14**, 9885–9891; (h) J. M. Posz, N. Sharma, P. A. Royalty, Y. Liu, C. Salome, T. C. Fessard and M. K. Brown, *J. Am. Chem. Soc.*, 2024, **146**, 10142–10149; (i) S. Hu, Y. Pan, D. Ni and L. Deng, *Nat. Commun.*, 2024, **15**, 6128; (j) R. Guo, Y.-C. Chang, L. Herter, C. Salome, S. E. Braley, T. C. Fessard and M. K. Brown, *J. Am. Chem. Soc.*, 2022, **144**, 7988–7994; (k) Y. Liu, S. Lin, Y. Li, J.-H. Xue, Q. Li and H. Wang, *ACS Catal.*, 2023, **13**, 5096–5103; (l) M. Xu, Z. Wang, Z. Sun, Y. Ouyang, Z. Ding, T. Yu, L. Xu and P. Li, *Angew. Chem., Int. Ed.*, 2022, **61**, e202214507; (m) N. Radhoff, C. G. Daniliuc and A. Studer, *Angew. Chem., Int. Ed.*, 2023, **62**, e202304771.
- Selected examples, see: (a) A. S. Harmata, T. E. Spiller, M. J. Sowden and C. R. J. Stephenson, *J. Am. Chem. Soc.*, 2021, **143**, 21223–21228; (b) T. Iida, J. Kanazawa, T. Matsunaga, K. Miyamoto, K. Hirano and M. Uchiyama, *J. Am. Chem. Soc.*, 2022, **144**, 21848–21852; (c) N. Frank, J. Nugent, B. R. Shire, H. D. Pickford, P. Rabe, A. J. Sterling, T. Zarganes-Tzitzikas, T. Grimes, A. L. Thompson, R. C. Smith, C. J. Schofield, P. E. Brennan, F. Duarte and E. A. Anderson, *Nature*, 2022, **611**, 721–726; (d) T. V. T. Nguyen, A. Bossonnet, M. D. Wodrich and J. Waser, *J. Am. Chem. Soc.*, 2023, **145**, 25411–25421; (e) Y. Zheng, W. Huang, R. K. Dhungana, A. Granados, S. Keess, M. Makvandi and G. A. Molander, *J. Am. Chem. Soc.*, 2022, **144**, 23685–23690.
- Selected examples, see: (a) V. V. Levterov, Y. Panasyuk, V. O. Pivnytska and P. K. Mykhailiuk, *Angew. Chem., Int. Ed.*, 2020, **59**, 7161–7167; (b) D. Dibchak, M. Snisarenko, A. Mishuk, O. Shablykin, L. Bortnichuk, O. Klymenko-Ulianov, Y. Kheylik, I. V. Sadkova, H. S. Rzepa and P. K. Mykhailiuk, *Angew. Chem., Int. Ed.*, 2023, **62**, e202304246; (c) V. V. Levterov, Y. Panasiuk, O. Shablykin, O. Stashkevych, K. Sahun, A. Rassokhin, I. Sadkova, D. Lesyk, A. Anisiforova, Y. Holota, P. Borysko, I. Bodenchuk, N. M. Voloshchuk and P. K. Mykhailiuk, *Angew. Chem., Int. Ed.*, 2024, **63**, e202319831.
- Selected examples, see: (a) Y. Tamura, H. Ishibashi, M. Hirai, Y. Kita and M. Ikeda, *J. Org. Chem.*, 1975, **40**, 2702–2710; (b) S. Breitenlechner and T. Bach, *Angew. Chem., Int. Ed.*, 2008, **47**, 7957–7959; (c) D. Albrecht, F. Vogt and T. Bach, *Chem.–Eur. J.*, 2010, **16**, 4284–4296; (d) A. Denisenko, P. Garbuz, N. M. Voloshchuk, Y. Holota, G. Al-Maali, P. Borysko and P. K. Mykhailiuk, *Nat. Chem.*, 2023, **15**, 1155–1163; (e) D. M. Whalley, L. Carlino, O. D. Putra, N. A. Anderson, S. C. Coote and O. Lorthioir, *Chem. Sci.*, 2024, **15**, 19564–19570.
- Selected reviews, see: (a) P. Bellotti and F. Glorius, *J. Am. Chem. Soc.*, 2023, **145**, 20716–20732; (b) J. Turkowska, J. Durka and D. Gryko, *Chem. Commun.*, 2020, **56**, 5718–5734; (c) Q.-B. Zhang, F. Li, B. Pan, S. Zhang, X.-G. Yue and Q. Liu, *Green Chem.*, 2024, **26**, 11083–11105; (d) A. Fawcett, *Pure Appl. Chem.*, 2020, **92**, 751–765; (e) C. B. Kelly, J. A. Milligan, L. J. Tilley and T. M. Sodano, *Chem. Sci.*, 2022, **13**, 11721–11737; (f) J. L. Tyler and V. K. Aggarwal, *Chem.–Eur. J.*, 2023, **29**, e202300008; (g) M. Golfmann and J. C. L. Walker, *Commun. Chem.*, 2023, **6**, 9; (h) Q. Q. Hu, J. Chen, Y. Yang, H. Yang and L. Zhou, *Tetrahedron Chem.*, 2024, **9**, 100070; (i) S. J. Sujansky and X. Ma, *Asian J. Org. Chem.*, 2024, **13**, 1–13.
- (a) Y. Liang, R. Kleinmans, C. G. Daniliuc and F. Glorius, *J. Am. Chem. Soc.*, 2022, **144**, 20207–20213; (b) Y. Liang, F. Paulus, C. G. Daniliuc and F. Glorius, *Angew. Chem., Int. Ed.*, 2023, **62**, e202305043.



- 11 (a) T. Qin, M. He and W. Zi, *Nat. Synth.*, 2024, **4**, 124–133; (b) T. Li, Y. Wang, Y. Xu, H. Ren, Z. Lin, Z. Li and J. Zheng, *ACS Catal.*, 2024, **14**, 18799–18809; (c) W. Wang, J.-A. Xiao, L. Zheng, W.-J. Liang, L. Yang, X.-X. Huang, C. Lin, K. Chen, W. Su and H. Yang, *Org. Lett.*, 2024, **26**, 10645–10650.
- 12 (a) S. Dutta, D. Lee, K. Ozols, C. G. Daniliuc, R. Shintani and F. Glorius, *J. Am. Chem. Soc.*, 2024, **146**, 2789–2797; (b) J. L. Tyler, F. Schäfer, H. Shao, C. Stein, A. Wong, C. G. Daniliuc, K. N. Houk and F. Glorius, *J. Am. Chem. Soc.*, 2024, **146**, 16237–16247.
- 13 M. Golfmann, M. Reinhold, J. D. Steen, M. S. Deike, B. Rodemann, C. Golz, S. Crespi and J. C. L. Walker, *ACS Catal.*, 2024, **14**, 13987–13998.
- 14 Selected examples, see: (a) K. Dhake, K. J. Woelk, J. Becica, A. Un, S. E. Jenny and D. C. Leitch, *Angew. Chem., Int. Ed.*, 2022, **61**, e202204719; (b) H. Wang, H. Shao, A. Das, S. Dutta, H. T. Chan, C. Daniliuc, K. N. Houk and F. Glorius, *Science*, 2023, **381**, 75–81; (c) S. Dutta, Y.-L. Lu, J. E. Erchinger, H. Shao, E. Studer, F. Schäfer, H. Wang, D. Rana, C. G. Daniliuc, K. N. Houk and F. Glorius, *J. Am. Chem. Soc.*, 2024, **146**, 5232–5241; (d) C. C. Chintawar, R. Laskar, D. Rana, F. Schäfer, N. Van Wyngaerden, S. Dutta, C. G. Daniliuc and F. Glorius, *Nat. Catal.*, 2024, **7**, 1232–1242; (e) F. Zhang, S. Dutta, A. Petti, D. Rana, C. G. Daniliuc and F. Glorius, *Angew. Chem., Int. Ed.*, 2025, e202418239; (f) J.-L. Zhou, Y. Xiao, L. He, X.-Y. Gao, X.-C. Yang, W.-B. Wu, G. Wang, J. Zhang and J.-J. Feng, *J. Am. Chem. Soc.*, 2024, **146**, 19621–19628; (g) W.-B. Wu, B. Xu, X.-C. Yang, F. Wu, H.-X. He, X. Zhang and J.-J. Feng, *Nat. Commun.*, 2024, **15**, 8005; (h) F. Wu, W. Wu, Y. Xiao, Z. Li, L. Tang, H. He, X. Yang, J. Wang, Y. Cai, T. Xu, J. Tao, G. Wang and J. Feng, *Angew. Chem., Int. Ed.*, 2024, **63**, e202406548; (i) H. He, F. Wu, X. Zhang and J. Feng, *Angew. Chem., Int. Ed.*, 2025, **64**, e202416741; (j) X. Wang, R. Gao and X. Li, *J. Am. Chem. Soc.*, 2024, **146**, 21069–21077; (k) Y. Liu, S. Lin, Z. Ding, Y. Li, Y. Tang, J. Xue, Q. Li, P. Li and H. Wang, *Chem*, 2024, **10**, 3699–3708; (l) Z. Lin, H. Ren, X. Lin, X. Yu and J. Zheng, *J. Am. Chem. Soc.*, 2024, **146**, 18565–18575; (m) J. Zhang, J. Y. Su, H. Zheng, H. Li and W. P. Deng, *Angew. Chem., Int. Ed.*, 2024, **63**, e202318476; (n) M. Zanini, A. Noble and V. K. Aggarwal, *Angew. Chem., Int. Ed.*, 2024, **63**, e202410207; (o) X.-G. Zhang, Z.-Y. Zhou, J.-X. Li, J.-J. Chen and Q.-L. Zhou, *J. Am. Chem. Soc.*, 2024, **146**, 27274–27281; (p) S. Dutta, C. G. Daniliuc, C. Mück-Lichtenfeld and A. Studer, *J. Am. Chem. Soc.*, 2024, **146**, 27204–27212.
- 15 (a) Y. Zhang, S. S. Chen, K. D. Li and H.-M. Huang, *Angew. Chem., Int. Ed.*, 2024, e202401671; (b) S.-Y. Tang, Z.-J. Wang, Y. Ao, N. Wang and H.-M. Huang, *Nat. Commun.*, 2025, **16**, 1354; (c) Y. Ao, N. Wang, S.-Y. Tang, Z.-J. Wang, L.-H. Zou and H.-M. Huang, *ACS Catal.*, 2025, **15**, 2212–2221.
- 16 Selected reviews, see: (a) L. Pitzer, J. L. Schwarz and F. Glorius, *Chem. Sci.*, 2019, **10**, 8285–8291; (b) H. Huang, P. Bellotti and F. Glorius, *Acc. Chem. Res.*, 2022, **55**, 1135–1147; (c) M. Kojima and S. Matsunaga, *Trends Chem.*, 2020, **2**, 410–426; (d) K. Ram Bajya and S. Selvakumar, *Eur. J. Org. Chem.*, 2022, **2022**, e202200229; (e) D. Kalsi, S. Dutta, N. Barsu, M. Rueping and B. Sundararaju, *ACS Catal.*, 2018, **8**, 8115–8120.
- 17 K. Gollnick and M. Weber, *Tetrahedron Lett.*, 1990, **31**, 4585–4588.
- 18 (a) N. A. Romero, K. A. Margrey, N. E. Tay and D. A. Nicewicz, *Science*, 2015, **349**, 1326–1330; (b) B. Chen, Y. Du and W. Shu, *Angew. Chem., Int. Ed.*, 2022, **61**, e202200773; (c) L. Pitzer, F. Sandfort, F. Strieth-Kalthoff and F. Glorius, *Angew. Chem., Int. Ed.*, 2018, **57**, 16219–16223.
- 19 J. B. McManus, N. P. R. Onuska and D. A. Nicewicz, *J. Am. Chem. Soc.*, 2018, **140**, 9056–9060.
- 20 Selected reviews, see: (a) A. Y. Chan, I. B. Perry, N. B. Bissonnette, B. F. Buksh, G. A. Edwards, L. I. Frye, O. L. Garry, M. N. Lavagnino, B. X. Li, Y. Liang, E. Mao, A. Millet, J. V. Oakley, N. L. Reed, H. A. Sakai, C. P. Seath and D. W. C. MacMillan, *Chem. Rev.*, 2022, **122**, 1485–1542; (b) K. L. Skubi, T. R. Blum and T. P. Yoon, *Chem. Rev.*, 2016, **116**, 10035–10074; (c) F.-D. Lu, J. Chen, X. Jiang, J.-R. Chen, L.-Q. Lu and W.-J. Xiao, *Chem. Soc. Rev.*, 2021, **50**, 12808–12827; (d) J. A. Milligan, J. P. Phelan, S. O. Badir and G. A. Molander, *Angew. Chem., Int. Ed.*, 2019, **58**, 6152–6163.
- 21 (a) Y.-L. Li, S.-Q. Zhang, J. Chen and J.-B. Xia, *J. Am. Chem. Soc.*, 2021, **143**, 7306–7313; (b) X. Jiang, H. Jiang, Q. Yang, Y. Cheng, L.-Q. Lu, J. A. Tunge and W.-J. Xiao, *J. Am. Chem. Soc.*, 2022, **144**, 8347–8354; (c) H. Jiang, X.-K. He, X. Jiang, W. Zhao, L.-Q. Lu, Y. Cheng and W.-J. Xiao, *J. Am. Chem. Soc.*, 2023, **145**, 6944–6952; (d) T. Liang, Y. Wu, J. Sun, M. Li, H. Zhao, J. Zhang, G. Zheng and Q. Zhang, *Chin. J. Chem.*, 2023, **41**, 3253–3260; (e) Y.-P. Shao and Y.-M. Liang, *ACS Catal.*, 2025, 1147–1157; (f) J. Hou, A. Ee, W. Feng, J.-H. Xu, Y. Zhao and J. Wu, *J. Am. Chem. Soc.*, 2018, **140**, 5257–5263.
- 22 X. Pan, H. Wang, C. Li, J. Z. H. Zhang and C. Ji, *J. Chem. Inf. Model.*, 2021, **61**, 3159–3165.
- 23 W. D. Jang, J. Jang, J. S. Song, S. Ahn and K. S. Oh, *Comput. Struct. Biotechnol. J.*, 2023, **21**, 3532–3539.
- 24 W. J. G. Hugh MacLean, *J. Physiol.*, 1928, **65**, 63–76.
- 25 L. Kong, X. Shu, S. Tang, R. Ye, H. Sun, S. Jiang, Z. Li, J. Chai, Y. Fang, Y. Lan, L. Yu, Q. Xie, W. Fu, Y. Wang, W. Li, Z. Qiu, J. Liu and L. Shao, *J. Med. Chem.*, 2022, **65**, 10377–10392.

